

Space grade fiber optic gyroscope: R&D results and flight tests

**Yu.N.Korkishko¹, V.A.Fedorov¹, V.E.Prilutskiy¹, V.G.Ponomarev¹, I.V.Morev¹,
A.I.Morev¹, D.V.Obuhovich¹, S.M.Kostritskii¹, A.I.Zuev¹, V.K.Varnakov¹,
A.V.Belashenko¹, E.N.Yakimov², G.V.Titov², A.V.Ovchinnikov², I.B.Abdul'minov²,
S.V.Latyntsev²**

¹ LLC RPC Optolink,
Moscow, Zelenograd, Sosnovaya alley, building 6a, premises 5, 124489
RUSSIA

² Academician M.F. Reshetnev Information Satellite Systems, Lenin Street,
Zheleznogorsk, Krasnoyarsk region, 662972
RUSSIA

Abstract

The aims of the current work are R&D and flight tests of fiber-optic gyro for space applications VOBIS. Space-grade FOGs VOBIS are developed for the tasks of spacecraft orientation and navigation at the high orbit and are long-life radiation resistant. Its' estimated operation time is 15 years in high vacuum and radiation environment.

1. Introduction

At present time fiber-optic gyroscopes (FOGs) with closed-loop feedback scheme of operation are becoming widely used in inertial navigation complexes. In FOGs with closed-loop scheme the feedback mechanism keeps the zero signal level by compensating the Sagnac phase shift with additional phase counter-shift. The value of the phase counter-shift allows one to obtain information about the angular rate of the device rotation [1].

Space satellites operate at high altitudes of 200-80000 km and carry out missions in the general areas of earth and space science, technology demonstration, remote sensing, commercial telecommunication and national defense. The mission of the satellite dictates the choice of the orbital path which may take it through Van Allen radiation belt and always radiated by cosmic rays.

The aims of the current work are the research and development and flight tests of fiber-optic gyro for space applications VOBIS. Space-grade FOGs VOBIS are developed for the tasks of satellite orientation and navigation at any orbit (flight tests performed in Geostationery orbit (GEO)) and are long-life radiation resistant. Its' estimated operation time is 15 years in high vacuum and radiation environment.

2. FOG VOBIS Configuration

2.1 Configuration

As part of the spacecraft (SC) developed by JSC "ISS" there are applied angular velocity sensors based on fiber-optic gyro (FOG). Device VOBIS (abbreviation in russian, fiber-optic angular velocity measurement unit) is designed and manufactured by LLC RPC "Optolink". Photo of the device is shown in Figure 1.

Device itself is a monoblock consisting of three autonomous orthogonally placed fiber-optic gyros, and is used for the tasks of space vehicle orientation and navigation at any orbit during its estimated operation time of 15 years in high vacuum and radiation environment.



Figure 1 - The appearance of the device VOBIS.

Angular rate measurement channels are independent so that a channel failure does not affect the other operational measurement channels by design.

Each optical measurement channel consists of a light source (superluminescent diode (SLD)) with optical fiber output from radiation-resistant single mode polarization-maintaining fiber, photodiode (PD) with optical fiber input from radiation-resistant multi-mode isotropic fiber, polariser-splitter (PS) on a LiNbO_3 chip with inputs and outputs made from radiation-resistant single mode polarization-maintaining fiber and a ring interferometer, sensitive to the angular rate of rotation (Figure 1). Blocks of electronics maintaining several functions such as power supply of FOG elements, photodiode signal processing and phase modulators control, are separated from the optical scheme. The measured angular rate data is output in the format of binary phase-manipulated code.

Thermal exchange of the device is performed through the base surface of mounting, the unit is qualified in temperature range $-30\text{ }^{\circ}\text{C}$ to $+40\text{ }^{\circ}\text{C}$.

The ring interferometer consists of a multifunctional integrated-optic chip (MIOC) performed on the substrate of LiNbO_3 , and of radiation-resistant polarization-maintaining optical fiber loop (FL). All elements of optical scheme with the exception of SLD and PD are serially produced by RPC "Optolink".

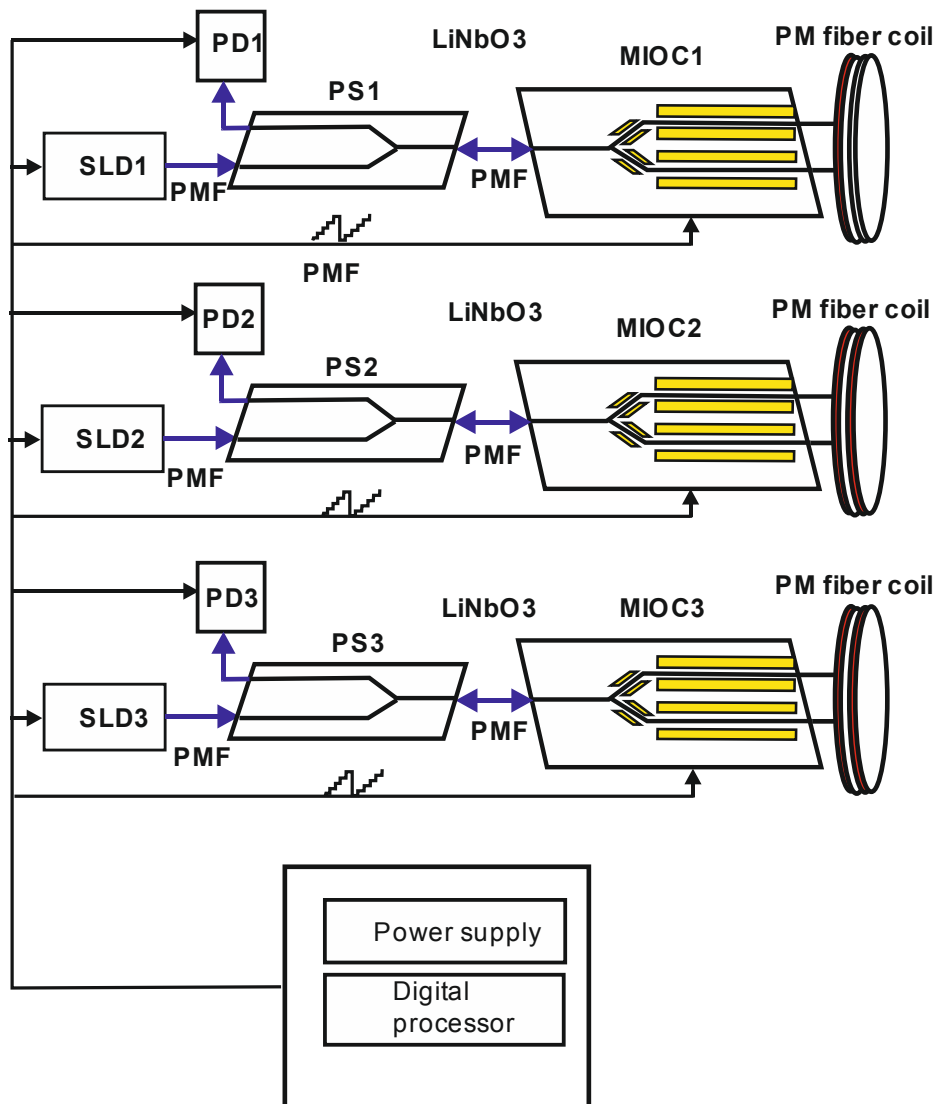


Figure 2. Configuration of FOG VOBIS.

2.2 Commercial Off The Shelf (COTS) components

We tried to minimize the number of purchased optical components in our FOG. VOBIS is comprising some of optical devices: active optoelectronic components (SLED, Receiver and MIOC), passive optical component (Polarising Splitter) and fiber coil for the Sagnac interferometer). As no space qualified alternative were available on the market, these optical devices were to be procured on commercial standard (Commercial Off The Shelf or COTS components) and upgraded to space standard. Fortunately, the main components (MIOC, PS, fiber coil and partially Receiver) are produced by Optolink. The SLEDs used are taken from the Telecom Industry, and some qualification data (such as Telcordia qualification) were already available. The objective is then to procure a batch of components and to qualify this batch with a representative sample. The qualification of the technology has been achieved in three steps: component procurement, qualification plan definition; qualification testing.

2.3 Radiation hard polarization maintaining fiber (PMF)

We have developed a technology for forming fluorine-doped silica glass light-reflecting cladding with $\Delta n \sim -(8.5 - 9.5) \times 10^{-3}$ using SiF_4 as fluorine-agent. After the fluorine-doped silica glass cladding deposition is finished inside the supporting tube, SiO_2 layers are deposited that form fiber core by SiCl_4 oxidation.

Optical fibers have been drawn out on drawing tower using a high-temperature graphite heater with simultaneous covering with protecting and strengthening two-layer UV-curable acrylo-urethane coating. Silica fiber diameter is $80 \pm 1,5 \mu\text{m}$.

Mode field diameter measured upon TIA standard equals $9.2 \pm 0.2 \mu\text{m}$ at $\lambda = 1.55 \mu\text{m}$. The refractive index profile is shown at Figure 3.

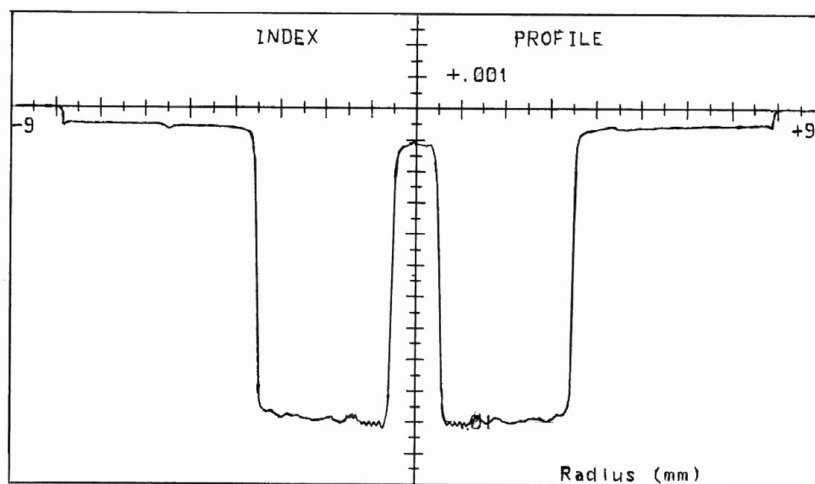


Figure 3. The refractive index profile of radiation hard polarization maintaining fiber.

Quadrupole winding technique implies winding a coil from a single segment of fiber, starting at the center of the segment, winding outward toward the ends, alternately from one or another of two supply spools, in a geometrically structured way. Indeed, optical fiber is elastic but very delicate. Elasticity implies a need to keep fiber always under constant tension during winding. Delicacy implies a need to control not only in-process fiber tension, but also fiber flexure or curvature, and a surface contact. The coil is placed at temperature isolated plate with diameter of 100 mm. Our fiber coil winding machine was specially developed basing on standard wire winding machine.

2.4 Integrated optical components

There are two LiNbO_3 integrated optical chips packed in one box. First is a passive polarization splitter (PS) and second is a multifunctional integrated optical chip (MIOC).

Both PS and MIOC are fabricated on X-cut LiNbO₃ substrate by High-Temperature Proton Exchange method (HTPE) [2]. PS has the same configuration as MIOC (Figure 2). It includes a linear polarizer and Y-junction coupler. MIOC is an active component and contains additionally two pairs of electro-optic phase modulators. Light coming from the SLED is linearly polarized within the PS and MIOC to greater than 60 dB polarization. This high degree of polarization minimizes bias uncertainty due to polarization non-reciprocity. The Y-junction coupler within the MIOC splits the light into equal amplitude waves, each directed along a separate waveguide within the MIOC. Each of the resulting waves pass through an electrooptical phase modulator and after two waves counterpropagate around the optical PM optical fiber sensor coil.

2.5 Electronics

Digital signal processor (DSP) generates voltage for “sawtooth” light modulation for compensation of Sagnac phase shift and to make fixed phase shift of $\pi/2$. As a result, each channel is working in closed-loop regime. Figure 4 shows the scheme of DSP.

Analog signal from the phase sensitive detector (PSD) that processes the output of the FOG photodetector is amplified and passed to high frequency analog to digital converter (ADC). The digital signal is demodulated by Altera Field Programmable Gate Array (FPGA). Obtained code passes to digital integrator. The code of signal from integrator is used to obtain the slope of phase “saw-tooth” which corresponds to rotation rate. The Digital to Analog converter creates the analog signal as saw-tooth voltage and passes it to MIOC. The wideband integrated optic phase modulators placed at both arms of MIOC are employed to introduce phase ramp modulation, thus enabling close-loop operation. The loop closure scheme uses a digitally synthesized saw-tooth (serrodyne modulation) of 2π amplitude in optical phase shift. In this case the Sagnac phase shift is compensated by saw-tooth modulation of light with calibrated amplitude 2π and frequency f , determined from well-known equation:

$$f = \frac{D}{n\lambda} \Omega$$

where Ω is a rotation rate, D – diameter of fiber coil, n - effective refractive index of waveguiding mode, λ - wavelength.

The frequency of resulting ramp is then a digital measure of the rotation rate, with each ramp reset proportional to the angular turned, i.e. one ramp is equal to $\frac{n\lambda}{D}$. To increase resolution of gyro the rotation rate is determined by measuring slope of phase saw-tooth.

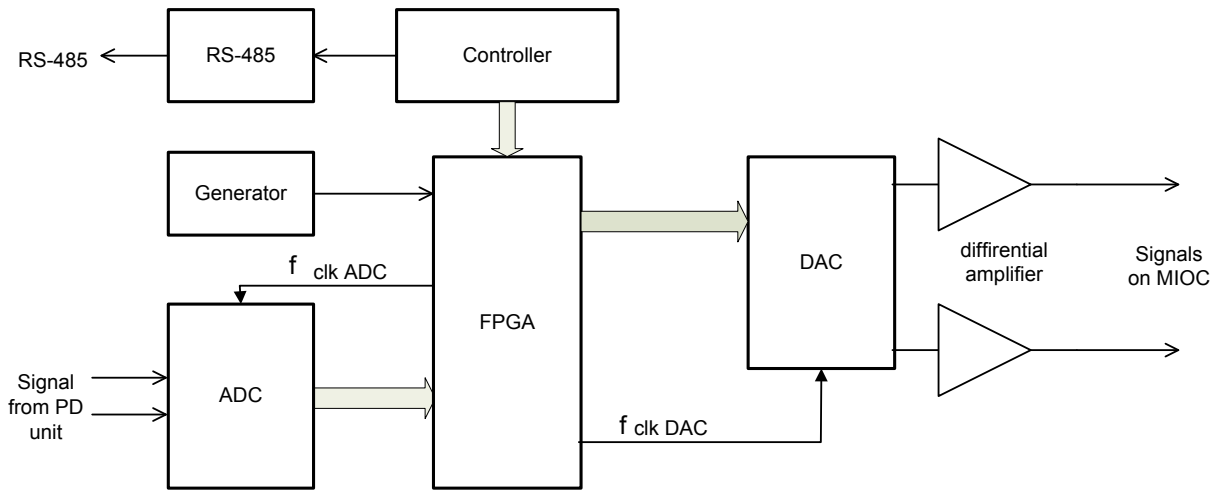


Figure 4. Block diagram of DSP. ADC – analog digital converter, DAC – digital analog converter, FPGA – Field Programmable Gate Array, PD unit – photodetector unit.

DSP represents the circuit based on Altera's FPGA. DSP is connected with high-speed ADC and with two fast Analog Devices's DAC. Clock pulse for DAC and ADC are drawing up by FPGA. Work of FPGA are clocked by external thermo-stabilized generator.

DSP uses the additional Atmel microcontroller which is working as the loader for FPGA. Controller provides an exchange with external devices via interface MIL STD 1553B. The monitor for device settings is realized based on this controller. Except for loading FPGA, the controller reads out the data of measurements from FPGA.

The shaper of clock pulses transforms clock frequency to a set of impulses for synchronous operation of all devices and units. Clock frequency f_{clk} gets out to multiple frequency AM f_{am} clock pulses for DAC that are formed on AM fronts. Clock pulses for ADC are formed so that to exclude measurements on fronts of a signal from PD.

The circuit of PD signal processing consists of the integration block, the buffer for storage of the measured value and the differencing circuit. The sum of the values of mismatch signal measured on the current phase AM is collected at integration block. On the buffer

the sum of the values measured on previous phase AM is stored. After the measurements the values from the integration block and from the buffer pass to the differencing circuit. Depending on current phase of AM, one number passes as deducted and another as the subtractor. Thus the amplitude of a variable signal is allocated taking into account its sign.

The code with sign, corresponding to a sign of a mismatch signal, passes to the digital integrator which consists of the multiplier and the summing unit with the circuit of restriction. The time constant of the digital integrator is set by the multiplier. The summing unit is used as the integrator. The code from the integrator passes to the shaper of the code for compensating modulation and through the digital filter to the serial interface of connection with the controller.

The shaper of a code for compensating modulation includes the summing unit which forms the "saw-tooth" code and the second summing unit which is used in a contour of a digital regulator of amplitude of compensating modulation. The signal from the circuit of processing of a signal from PD taken off at the moment of recessions of "saw-tooth" serves as signal of a mismatch for a digital regulator of amplitude of compensating modulation. The same signal is used for the fine tuning of auxiliary modulation amplitude.

There are two main sources of scale factor errors: (i) the finite flyback time and (ii) the nonstability of phase amplitude. To avoid influence of first factor we used the special transformation in the circuit, which creates a control voltage signal for MIOC. In our scheme the flyback time is excluded from transmission characteristics of electro-optical modulator. The nonstability of phase amplitude is minimized by creating the astatic follow-up system. The response of device on periodic signal with calibrated constant period is considered as an error signal. Special circuit, independently on FOG moving, generates this periodic signal securing the zero error of stabilization of phase saw-tooth at 2π value at stationary rate and negligibly small error of this value at dynamic rate.

3. FOG VOBIS performance

3.1 Main requirements and specifications for VOBIS

Main requirements and specifications for VOBIS device are shown in Table 1.

Table 1. Main requirements and technical characteristics of VOBIS device

Parameter	Value
Range of measured angular rate, °/s	±30
Range of linear angular rate measurement zone, °/s	±15
Scale factor error, %	±0,05
Bias constant error, °/h	±1
Bias instability in 12-hours test at constant temperature, averaging time $\tau = 100$ s, less than, °/h (1σ)	±0,03
Bias instability in operational temperature range with temperature change rate $< 0,15$ °C/min, averaging time $\tau = 100$ s, less than, °/h (1σ)	±0,3
Weight, kg	2,7
Estimated lifetime, hours	140 000
Temperature range of mounting surface, °C	- 30 ... +40
Voltage, V	23...28
Power supply, W	25
Data exchange interface	MIL STD 1553B

The main stages of the device life cycle on which its performance can be evaluated - production, acceptance test in the operating organization, ground testing as part of the spacecraft, and normal operation as part of the spacecraft in orbit. At each stage of mentioned life cycle the device operation and its accuracy parameters are checked with the registration of all output.

3.2 Environmental Parameters

During the ground experimental testing VOBIS passed all the necessary tests to confirm its characteristics and resistance to external factors.

Device VOBIS successfully passed the following tests:

- low-frequency interference resistance;
- high-frequency interference resistance;
- resistance to impulse noises;
- susceptibility to electric field;
- susceptibility to constant magnetic field;
- operability tests in the conditions of vacuum with the varying mounting platform temperature in range from -40°C to $+50^{\circ}\text{C}$;
- operability tests after the pressure reduction from normal to vacuum within the time 100s;
- accelerated life tests (140000 h) and tests on persistence (20 years);
- tests on the optical channel resistance to the impact of ionizing radiation with the total cumulative dose of radiation up to 1100 kRad.
- tests on optical elements (MIOC, fiber-optic loop, PD, SLD) resistance to the effects of biasing when exposed to high-energy protons with fluency $2 \cdot 10^{12}$ proton/cm²;
- test on the resistance to the γ -radiation. The device passed through 8 γ -pulses with duration 200 ns with increasing power from 10^7 R/sec to 6×10^{10} R/sec.
- test on broadband vibration impact in range 20-2000 Hz;
- test on shock impact with peak accelerations up to 300 g;
- test on vehicles.
- test on random vibration in range 20-2000 Hz;
- test on shock with peak accelerations up to 300 g;
- test on vehicles.

The operation time of VOBIS was estimated 15 years.

3.3 *Laboratory tests*

After VOBIS devices were delivered to the operating organization (JSC "ISS") devices were tested on a stable basis in the normal climatic conditions lasting for 12 hours for each axis in vertical orientation ("straight up"). The change in temperature during the test resulted to 0,3 ... 0,7 ° C for the device VOBIS1 and 0,8 ... 1,5 ° C for VOBIS2 device. The results of parameters estimation are shown in Table 2.

Table 2. Results of VOBIS devices parameters evaluation during acceptance control test

Parameter	Axis X	Axis Y	Axis Z
Noise level (1σ), $^{\circ}/h$			
– VOBIS1	0,31	0,34	0,38
– VOBIS2	0,34	0,40	0,40
Bias signal change in tests, $^{\circ}/h$			
– VOBIS1	0,03	0,03	0,04
– VOBIS2	0,04	0,08	0,06
Bias instability, averaging time $\tau = 100$ s, $^{\circ}/h$			
– VOBIS1	0,015	0,018	0,019
– VOBIS2	0,016	0,025	0,026

The estimation value of the angular rate noise level is given by Allan variance (1σ) at the point of averaging time equal to sampling period of 0,25 seconds (sampling rate – 4 Hz) [5,6].

Figure 5 shows Allan variance for VOBIS-1 obtained during acceptance test at laboratory.

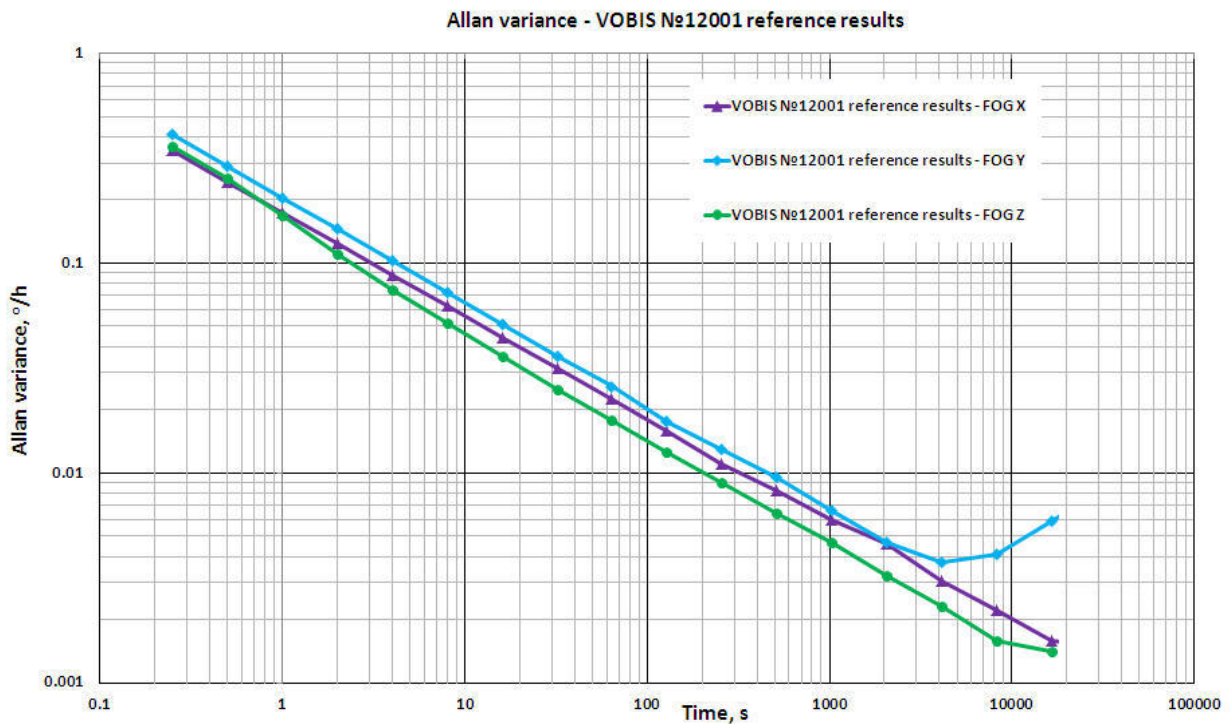


Figure.5 Allan variance for VOBIS obtained during acceptance test at laboratory.

3.4 Ground tests as part of the spacecraft

At the stage of spacecraft ground tests, the spacecraft is undergoing numerous checks including thermal vacuum chamber tests, which allows to testing the thermal control system and comprehensive equipment inspection at the borders of temperature range. The width of the temperature change range outside the machine during the test was 70 °C, but for VOBIS devices inside the spacecraft chassis, the observed temperature change range was just over 40 °C. According to the estimate of temperature sensors temperature values inside the VOBIS devices, the device mounting surface temperature during the test varied in range from -10 °C to + 30° C. Maximum rate of temperature change in the tests was 0,32 °C/min. The results of devices' parameters estimation are shown in Table 3

Table 3. Results of VOBIS devices parameters evaluation during ground tests as part of the spacecraft

Parameter	Axis X	Axis Y	Axis Z
Noise level (1σ), °/h			
– VOBIS1	0,55	0,65	1,11
– VOBIS2	0,62	0,73	0,68
Bias signal change in tests during the temperature change at rate 0,3 °C/min, °/h			
– VOBIS1	0,30	0,66	0,48
– VOBIS2	0,60	0,60	0,96
Bias instability, averaging time $\tau = 100$ s, °/h			
– VOBIS1	0,026	0,084	0,046
– VOBIS2	0,182	0,047	0,074

3.5 Flight tests

On 28th September 2014 there was performed a successful launch of Russian GEO telecommunication satellite “Luch” (“Luch” means Beam (Ray)) with installed two space-grade fiber-optic gyroscopes VOBIS-1 and VOBIS-2.

Initial orientation modes of the spacecraft using VOBIS devices were correctly performed, the main and reserved VOBIS devices during checks operated correctly. No functioning not performance anomaly was detected up to now. The performances of both gyroscopes VOBIS-1 and VOBIS-2 are very close, so we give results for VOBIS-1 only.

3.5.1 Tests after 1-year operation at the GEO orbit

According to the results of one year of operation in November 2015 there was held control evaluation of VOBIS devices' parameters. According to temperature sensors installed in the device, daily temperature fluctuations are no more than 2 °C, the temperature change rate does not exceed 0.03 °C/min. The results of parameters evaluation in 24-hour test are given in Table 4.

Table 4. Results of VOBIS devices parameters evaluation after 1-year operation in GEO

Parameter	Axis X	Axis Y	Axis Z
Noise level (1σ), °/h			
– VOBIS1	0,46	0,40	0,76
– VOBIS2	0,53	0,43	0,56
Bias signal change in tests during the 24-hours temperature change 2 °C, °/h			
– VOBIS1	0,1087	0,0708	0,1342
– VOBIS2	0,1021	0,1516	0,2668
Bias instability, averaging time $\tau = 100$ s, °/h			
– VOBIS1	0,0260	0,0180	0,0382
– VOBIS2	0,0277	0,0211	0,0577

Figure 6 shows Allan variance for VOBIS-1 obtained during 24 hours run in December 2015 after a 15-months flight. The sampling rate was 4 Hz. For channels X and Y one can see the periodic oscillations with period around 3 seconds which corresponds to oscillations of solar panels.

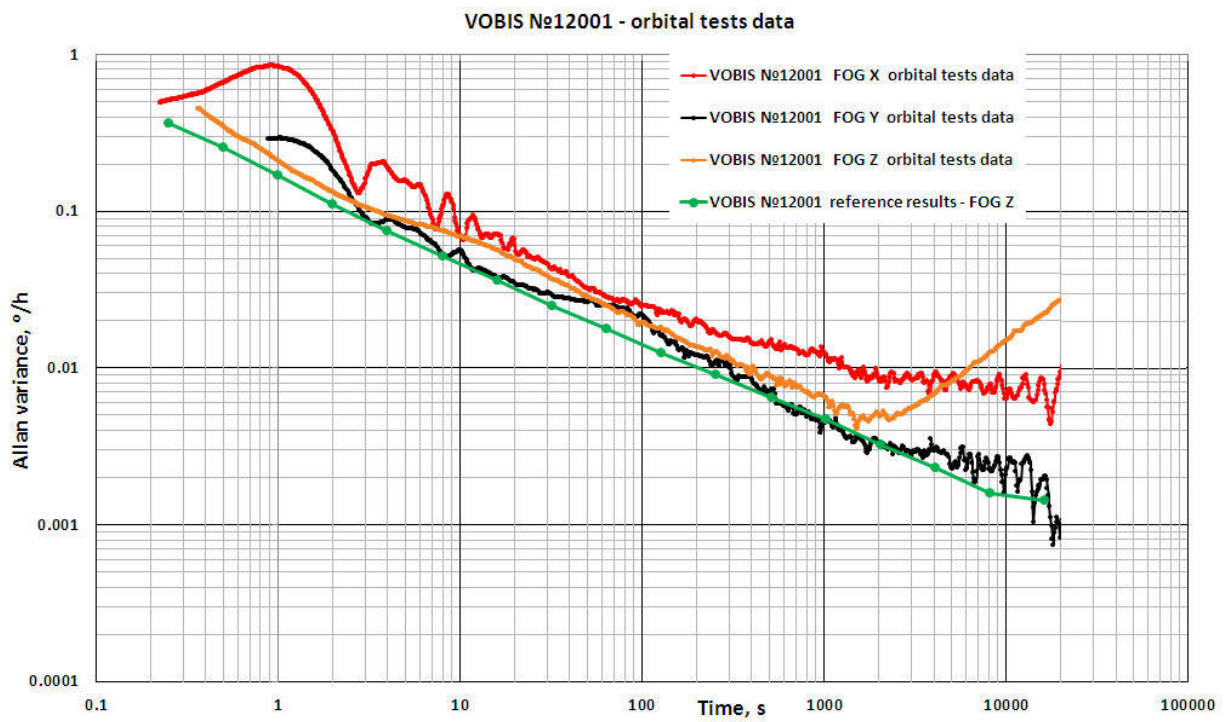


Figure 6. Allan variance for VOBIS obtained during flight test after 12-months flight in GEO.

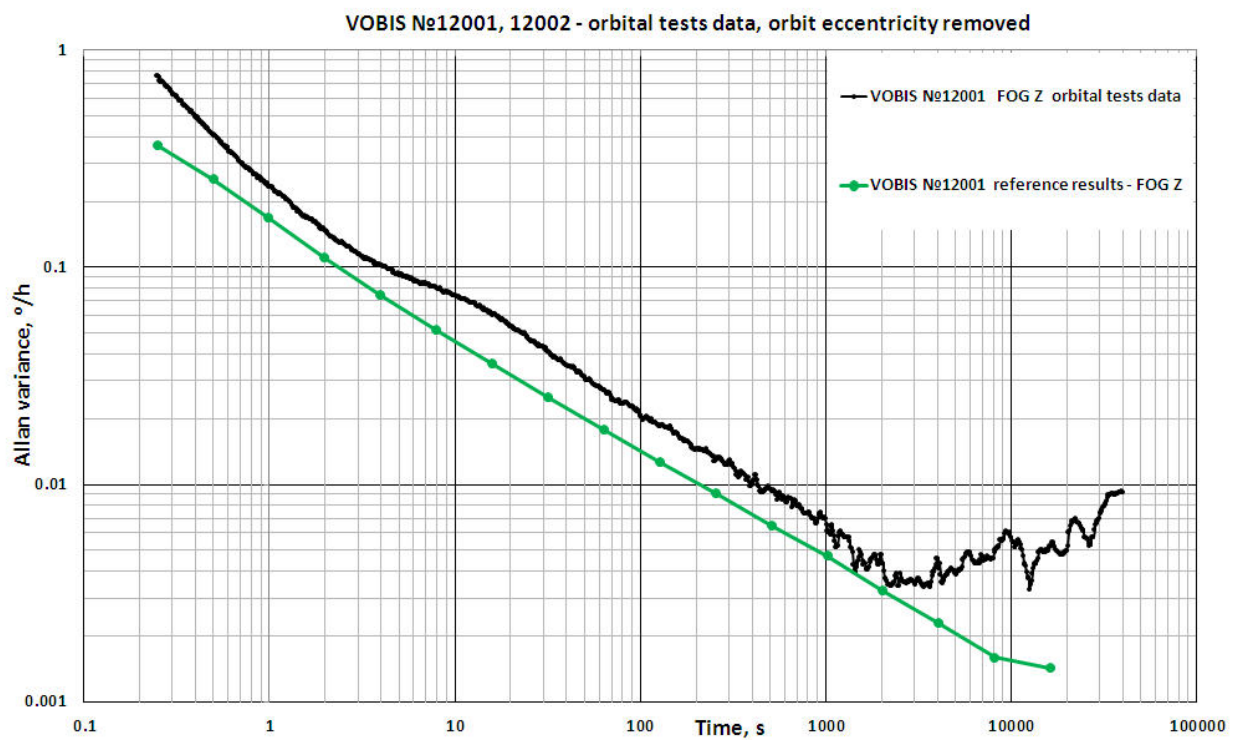


Figure 7. Allan variance for Z-axis of VOBIS after filtering the eccentricity.

3.5.2 Tests after 21-month operation at the GEO orbit

In July 2016 there was carried out another regular check of VOBIS parameters. Daily temperature fluctuations correspond to the values obtained in November 2015. The results of parameters evaluation are given in Table 5.

Table 5. Results of VOBIS devices parameters evaluation after 21-month operation in GEO orbit

Parameter	Axis X	Axis Y	Axis Z
Noise level (1σ), $^{\circ}/h$			
– VOBIS1	0,45	0,45	0,99
– VOBIS2	0,52	0,43	0,70
Bias signal change in tests, temperature change in tests $2^{\circ}C$, $^{\circ}/h$			
– VOBIS1	0,155	0,416	0,217
– VOBIS2	0,159	0,441	0,254
Bias instability, averaging time $\tau = 100$ s, $^{\circ}/h$			
– VOBIS1	0,039	0,049	0,071
– VOBIS2	0,040	0,058	0,076

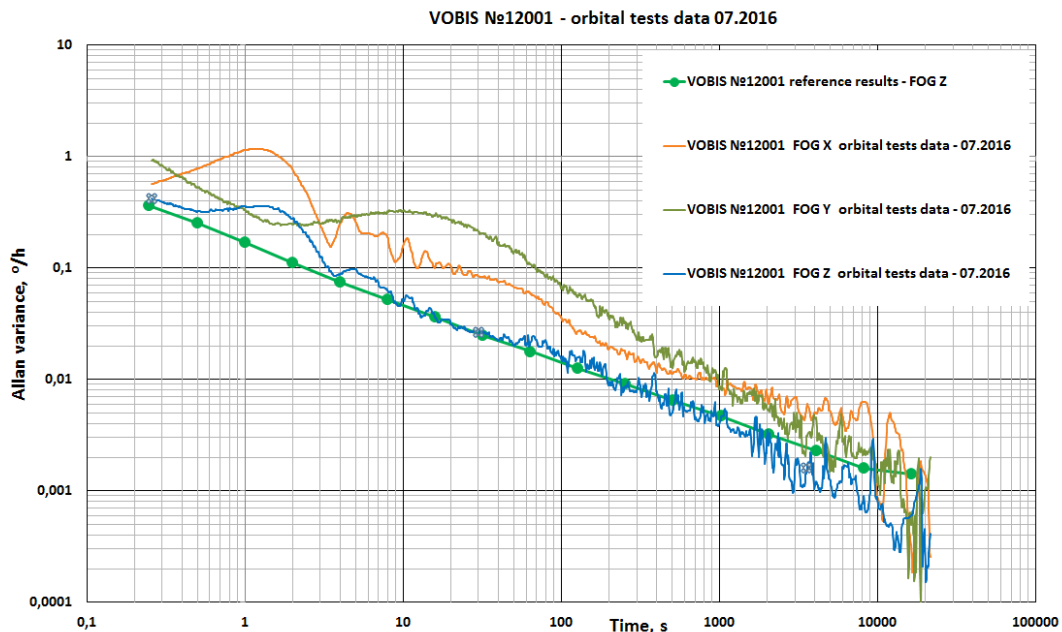


Figure 8. Allan variance for VOBIS obtained during flight test after 21-months flight in GEO.

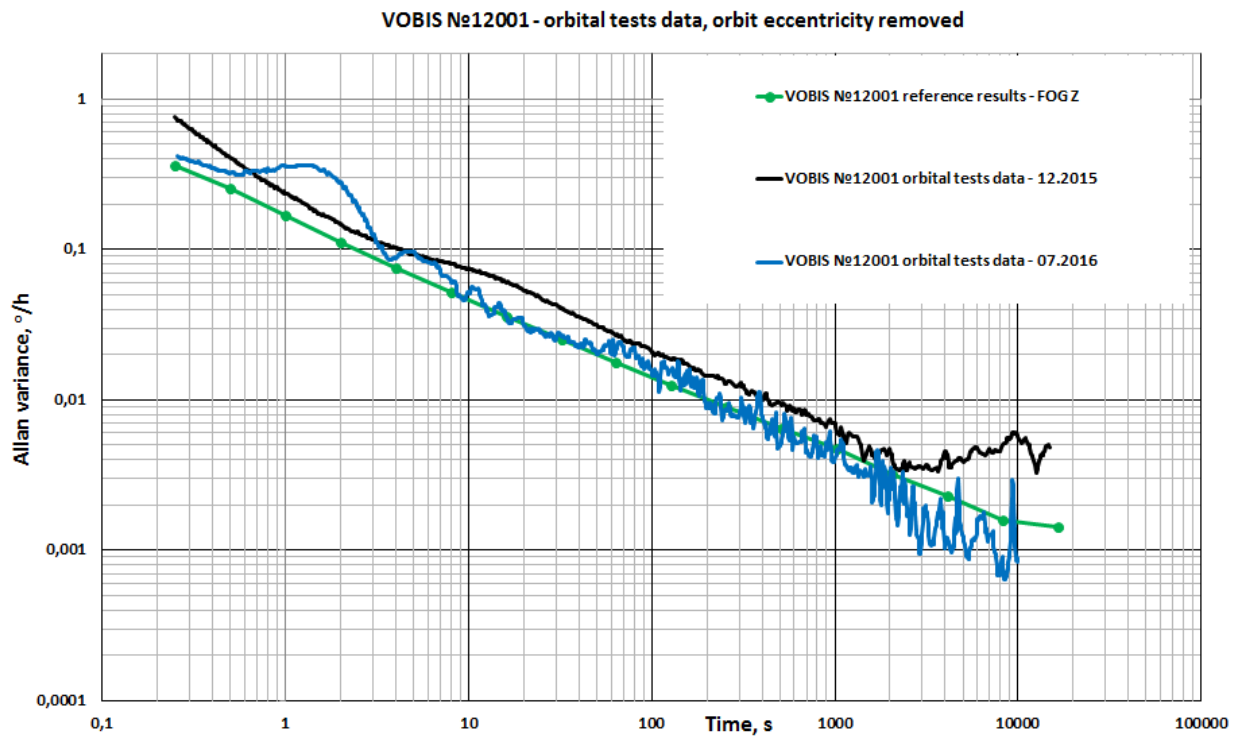


Figure 9. Allan variance for Z-axis of VOBIS after filtering the eccentricity after 21-months flight in GEO.

4. Results and discussion

4.1 Noise level

The factory equipment tests are carried out in climatic chambers, the observed gyro noise level in these tests is different from run to run and is in range 0,4 to 2,0 °/h (1σ). The reason for this variation is the effect of workplace noise: when running on an isolated basement the measured noise has a stable value in the range of 0.3 to 0,4 °/h (1σ) for all measurement channels. When the testing takes place in a climatic chamber the vibration from the workplace and other equipment is transferred to the device. This effect is observed in the increased level of the device angular rate variations in the chart and also in the form of "saw" in Allan variation graphs within the averaging time range of 0.25 ÷ 5 seconds (Figures 6, 8, 9). When testing the device on a stable basis (isolated basement) "saw" is absent (Figure 5). The ground test results as a part of SC and the noise level is higher than in the case of isolated basement. Most likely, this is due to the mechanical interaction between the device chassis and the workplace (thermal vacuum chamber) through the spacecraft hull and the workplace high noise.

When comparing the graphs Allan variance for these two cases, it is clear that the vibration effect on the device signal does not exert any significant influence for the

averaging times over a period of 10 seconds. This case demonstrates the need for studying the entire frequency spectrum of the device signal during the inspections as the preliminary data averaging before the parameters evaluation may result into untimely identification of the defect, which may affect the performance of control system.

As a result of 1-year successful operation in the conditions of outer space the devices' angular rate values demonstrate the noise levels convergence for the measurement channels whose axes are collinear, the noise level for X and Y axes does not exceeded $0,5^{\circ}/h$ (1σ), which corresponds to the values obtained during ground tests. The axes Z show slightly higher noise level due to the spacecraft vibrations caused by the operation of solar panels drive.

4.2 *Bias signal*

At all stages of the life cycle zero signal value does not exceed the tolerance of $\pm 1^{\circ}/h$. The logic of the spacecraft control system enables the ability of VOBIS automatic zero angular rate calibration with reliance upon star sensors data during the operation of the spacecraft in orbit. Zero signal values calculated from 24-hours inspection in July 2016, the results differ from the last calibration (January 2016) no more than $0,001^{\circ}/hr$. It is expected that the value of the VOBIS measurement channels zero signal has stabilized and will not change further. Dynamics of this parameter in time will be further observed.

4.3 *Allan variance*

The graphs plotted on the basis of flight operations data in 2015 and in 2016 indicate the presence of periodic processes in channels X and Y with a period of about 3 seconds. Such period corresponds to the period of the spacecraft mechanical systems vibrations - solar panels, antenna etc.

VOBIS1 unit data for year 2015 shows the influence of the orbit eccentricity on the Allan curve. After taking into account the orbit eccentricity influence new Allan variance curve was plotted (Figure 4).

On the basis of obtained data the following factors are assumed to influence the VOBIS performance parameters: the eccentricity of the orbit, works done to carrying out corrections and unloading flywheels, vibration from the operation of SC mechanical system - flywheel system and solar panels rotation drives as well as the construction self-oscillation, which contributed to the values of the parameters listed in the tables. In view of this facts, VOBIS parameters evaluation in the course of flight operations should be carried

out taking into account the operating conditions of equipment, control systems and orbital motion of the spacecraft.

4.4 *Optical characteristics*

It is known that the regular optical fiber transmissivity significantly decreases due to degradation under strong ionizing radiation. Therefore, in this case in order to ensure the proper light level on PD the SLD pumpung current should gradually increase with fiber degradation. In addition, if exceeding the limit of SLD current the SLD load increases manifold with consequent shortening of its operation lifetime. This fact results in futher SLD failure and VOBIS failure in overall.

Measurements of SLD current after 20-months operation in GEO have indicated that the SLD current value is almost equal to values measured during devices' manufacturing, and no reasonable current increase is obseved under the accumulated radiation dose. This clearly demonstrated high radiation hardness of VOBIS optical scheme and of VOBIS units in overall.

5. **Conclusion**

Interferometric Fiber Optics Gyroscopes are ideal candidates as robust, all solid state, high reliability inertial sensors. New FOG VOBIS has been developed for space application. The gyro is tolerant to high radiation and vacuum. Extensive tests verified the gyro performance and demonstrated low noise characteristics ($ARW < 0,005 \text{ deg}/\sqrt{\text{hr}}$).

The gyros demonstrated in run bias stability better than 0,03 deg/hr. Performed tests shown no degradation of VOBIS accuracy parameters after 21-months flight in GEO. Such performance makes this gyro suitable for many defense and space application. Further variations of the gyro are being considered to meet specific customer demands.

References

- [1] Lefevre H., The Fiber-Optic Gyroscope, Artech House, 1993.
- [2] Y.N.Korkishko, V.A.Fedorov, and O.Y. Feoktistova, LiNbO₃ optical waveguide fabrication by high-temperature proton-exchange, IEEE J. Lightwave Technol., 2000,.vol.18, pp.562-568.
- [3] P.G.Suchoski, T.K.Findakly, and F.J. Leonberger, Stable low-loss proton-exchanged LiNbO₃ devices with no electro-optic degradation, Opt. Lett., 1988, vol.13, pp.1050-1052.

- [4] Y.N.Korkishko and V.A.Fedorov, Structural Phase Diagram of $H_xLi_{1-x}NbO_3$ waveguides: The Correlation Between Structural and Optical Properties, IEEE Journal of Selected Topics in Quantum Electronics, 1996, vol.2, pp. 187-196.
- [5] J.L. Davis, and S. Ezekiel, Techniques for shot noise limited inertial rotation measurement using a multiturn fiber Sagnac interferometer, Proc.SPIE, 1978, vol.157, pp.131-137.
- [6] IEEE Standard Specification Format Guide and Test Procedure for Single-Axis Laser Gyros. IEEE Std 647-2006.
- [7] Yu.N.Korkishko, V.A.Fedorov, V.E.Prilutskiy, V.G.Ponomarev, I.V.Morev, D.V. Obuhovich, I.V.Fedorov, N.I.Krobka. Investigation and Identification of Noise Sources of High Precision Fiber Optic Gyroscopes// in Proc. 20th Saint Petersburg International Conference on Integrated Navigation Systems, Saint Petersburg, May 27-29, 2013, pp.59-62.